Published in final edited form as:
J Surg Res. 2012 July ; 176(1): 348–358. doi:10.1016/j.jss.2011.07.054.

The Role of Osteopontin and Osteopontin Aptamer (OPN-R3) in Fibroblast Activity

Cedric Hunter, BS[1,**], **Jennifer Bond, PhD**[1,**], **Paul C. Kuo, MD, MBA, FACS**[2], **M. Angelica Selim, MD**[3], and **Howard Levinson, MD, FACS**[1,3,*]

[1]Division of Plastic and Reconstructive Surgery, Department of Surgery, Duke University Medical Center, Durham, North Carolina

[2]Division of General Surgery, Department of Surgery, Loyola University Health System, Chicago, Illinois

[3]Department of Pathology, Duke University Medical Center, Durham, North Carolina

Abstract

Background—Scarring is believed to be caused by both persistent inflammation and overexuberant fibroblast activation. Osteopontin (OPN) is a cytokine that promotes cell activation. The absence of OPN *in vivo* reduces dermal scarring. This suggests that OPN is involved in scar formation; however, how OPN exerts these pro-scarring effects is unknown. RNA aptamers are short RNA molecules that bind target proteins with high affinity. The aptamer OPN-R3 (R3) blocks OPN signaling. The role of R3 in preventing dermal fibrosis is unknown.

Methods—Fibroblast migration was analyzed with the use of Boyden Chambers and HEMA-3 staining. Inverted confocal microscopy was used to assess fibroblast focal adhesion length. Adhesion was measured by incubating fluorescently stained fibroblasts on OPN coated 96-well plates. CellTiter 96® AQueous Non-Radioactive Cell Proliferation Assay was utilized to investigate the proliferative activity of fibroblasts. Free floating collagen lattices were utilized to assess fibroblast contractility.

Results—Human dermal fibroblasts migrated significantly in response to OPN. OPN did not induce a significant increase in focal adhesion length compared to controls. Adhesion studies demonstrated that OPN increased fibroblast adhesion. Proliferation assays indicate that OPN increased fibroblast growth. OPN increased fibroblast contractility of collagen lattices. The addition of R3 significantly inhibited OPN induced activity.

Conclusion—OPN is associated with scar and exerts pro-scarring effects by increasing cellular migration, adhesion, proliferation, and contractility of human dermal fibroblasts. R3 prevents OPN mediated activity. OPN may be useful for promoting closure of non-healing wounds and the OPN specific aptamer, R3, may be useful for preventing fibrosis.

[*]To whom correspondence and reprint requests should be addressed at Division of Plastic Surgery, Department of Surgery, Duke University Medical Center, Mail Location: Box 3974 Med Ctr, Durham, NC 27710.howard.levinson@duke.edu. Telephone number: 919-684-8661. Fax number: 919-684-5928.
[**]Co first authors.

Keywords

osteopontin; aptamer; wound healing; fibroblasts

INTRODUCTION

Fibrocontractile disease is ubiquitous throughout the human body and has a wide range of etiologies including idiopathic, infectious, and traumatic. There are at least 44 million patients per annum in the United States and 42 million patients in the EU who would benefit from pharmaceuticals that prevent or reduce scarring, most of whom are poor and underserved (1). Current therapies such as surgery, steroid injections, and pressure garments are marginally effective because they do not adequately address the molecular causes of scarring. For more effective patient care we need to develop better anti-scarring approaches. To fill this void, we must first better understand the biology of what causes fibrosis and scar contracture.

Wound healing is a complicated process composed of three phases: the inflammatory phase, the proliferative phase, and the remodeling phase. Neutrophil and macrophage infiltration along with hemostasis are notable features of the initial inflammatory phase. Once debridement has occurred and a scaffold for cellular migration has been created the proliferative phase of repair is observed as fibroblasts invade, increase their density by proliferation, and become the major synthetic cell producing a collagen rich connective tissue matrix (2). During the remodeling phase, the collagen rich granulation tissue is crosslinked and contracted by cell contractility into a scar with dense, compact collagen fibers (2). This complex process is mediated by various growth factors and signaling molecules that play critical roles in the pro-fibrogenic and pro-inflammatory reactions that under certain conditions result in excessive fibrosis (3). Currently, scarring is believed to be caused by prolonged inflammation, persistent cytokine stimulation, and overexuberant fibroblast activation with attenuated apoptosis and senescence (4, 5).

Osteopontin (OPN) is a secreted phospho-protein containing an Arg-Gly-Asp binding motif that interacts with cell surface receptors $\alpha_v\beta_3$-integrin and CD44, as well as extracellular matrix elements, fibronectin (6–9). OPN is synthesized by various immune cells including macrophages, dendritic cells, and natural killer cells (10). OPN binds to extracellular receptors and activates cell signaling pathways, such as the phosphorylation of focal adhesion kinase (FAK), paxillin, tensin, and Src, which initiate the OPN mediated cell-cell and cell-matrix interactions (11–15). OPN is involved in several diverse physiological and pathological processes including bone remodeling, cancer metastasis and invasiveness, inhibition of apoptosis, inflammation, and wound healing (7, 11, 12, 16). Recent studies have demonstrated the pro-fibrotic effects of OPN. OPN is highly expressed in human idiopathic pulmonary fibrosis and induces a significant increase in migration and proliferation of both lung fibroblasts and epithelial cells. Studies examining kidney fibrosis have seen similar findings demonstrating that OPN enhances renal scarring after an acute ischemic event (17, 18). In the absence of OPN, fibrosis and scarring are reduced. Studies using rodent models of pulmonary fibrosis have also reported a reduction in collagen type I deposition after bleomycin sulfate treatment in the absence of OPN (16, 19). Dermal wound studies in OPN-null mice have demonstrated that OPN knockout mice have a disorganized matrix with haphazardly arranged collagen fibrils composed only of homogenous smaller diameter fibrils whereas control OPN wild-type mice collagen fibrils are organized into fine well defined fibers composed of heterogeneous fibrils of varying diameter (20). These studies indicate that OPN clearly has a role in tissue fibrosis and that blockade of OPN may be a means to reduce scarring.

Small single-stranded RNA aptamers specifically bind to target proteins with high affinity and inhibit their function (11). Aptamers are stable and lack immunogenicity, making them an attractive alternative therapy to other small molecules. An apatmer to OPN, has been characterized (11). The OPN apatmer, OPN-R3 was shown to have a *K*d of 18 nmol/l and binds specifically to human OPN as determined by RNA electrophoretic mobility assays (11). Studies involving MDA-MB231 human breast cancer cells have demonstrated that an OPN-directed RNA aptamer (OPN-R3) decreased *in vitro* cellular adhesion, migration, and invasion by 60, 50, and 65%, respectively. In addition to decreasing *in vitro* activity, OPN-R3 decreased *in vivo* local tumor progression and distant metastases (11, 21). The role of OPN-R3 in preventing dermal fibrosis has not been investigated.

This study aims to investigate the role of OPN and the OPN inhibitor, OPN-R3, in wound healing and fibrosis through its effects on human dermal fibroblast migration, proliferation, adhesion, focal adhesion (FA) size, and contractility. We hypothesize that (1) OPN promotes dermal fibrosis by increasing dermal fibroblast motility, focal adhesion length, adhesion, proliferation, and contractility, and that (2) OPN induced effects are significantly inhibited in the presence of the OPN-R3 RNA aptamer.

MATERIALS AND METHODS

Cell Culture

Normal skin fibroblasts were explanted from four different human patients. Tissue specimens were obtained from the operating room as per Duke University Medical Center Institutional Review Board approval. In brief, tissues were washed, finely minced, and incubated in collagenase type I and DMEM (Sigma-Aldrich; St. Louis, MO) with 1% penicillin/streptomycin at 37ºC and 5% CO_2 for 4 h. The cells were subsequently collected as a pellet via centrifugation at 200g for 5 min, and cultured in DMEM supplemented with 10% Fetal Bovine Serum (FBS, Invitrogen; Carlsbad, CA) and 1% penicillin/streptomycin. Cells were fed three times weekly and passaged by trypsinization at confluence. Cultures were maintained in a humidified incubator with the same settings as mentioned above. Experiments with primary cell cultures were performed when cells were 80–90% confluent and cells were between passage numbers 1–9.

In vitro Migration Assay

Migration was assessed using a modified Boyden chamber assay. Briefly, the wells of a 24-well tissue culture treated plate (Corning Inc.; Corning, NY) were filled with 750 μl of DMEM containing the appropriate concentration of OPN (R&D Systems, Inc; Minneapolis, MN). Collagen coated PET-etched polycarbonate cell migration inserts (8 μm pores; BD Falcon; Franklin, NJ) were carefully placed into the medium containing wells. Human dermal fibroblasts were resuspended in DMEM serum-free medium at a concentration of 5×10^4 cells/ml in the presence or absence OPN-R3; 500 μl of this cell suspension was added to each insert. The modified chamber was then placed in a humidified incubator at 37ºC and 5% CO_2 for 22 h, after which the upper surface of the insert was swabbed to remove non-migratory cells. Migrated cells were then fixed and stained using the Protocol HEMA-3 cell staining kit (Fisher Diagnostics; Middletown, VA). The membrane was then removed from the insert and placed between a glass slide and coverslip. Migration was quantified by counting the number of cells in 5 random high power fields (HPF) at 200x magnification under a light microscope.

Immunofluorescence, Microscopy, and Image analysis

Focal adhesion size was assessed using immunofluorescence and confocal microscopy. Briefly, the chambers of an 8 well chamber slide system (Nunc, Inc.; Rochester, NY) were

filled with 250 μl of carbonate buffer (pH 9.6) containing either 50 nM OPN alone or 50 nM OPN plus 500 nM OPN-R3. The chamber system was placed overnight at 4ºC. Wells were rinsed with PBS (Invitrogen; Carlsbad, CA), and non-specific binding sites were blocked via the addition of 1% bovine serum albumin (BSA) in PBS for 1 h at 37ºC and 5% CO_2. Human dermal fibroblasts were resuspended in DMEM serum-free medium at a concentration of 1×10^5 cells/ml; 200 μl of cell suspension was added to each well. Chamber systems were incubated overnight at 37ºC and 5% CO_2. Cells were then rinsed with PBS and fixed with 4% paraformaldehyde for 15 min followed by 3 washes with PBS. Cells were then permeabilized with 0.3% Triton X-100 (Sigma-Aldrich; St. Louis, MO) for 5 min, and then blocked with 1% BSA for 30 min. Cells were incubated for 1 h at room temperature with primary antibody, mouse monoclonal anti-vinculin primary IgG1 (Sigma-Aldrich; St. Louis, MO), 1:400 in 1% BSA-PBS solution followed by three, 5 min PBS washes. Cells were then incubated for 1 h at room temperature with secondary antibody, Alexa Fluor® 568 goat anti-mouse IgG1 (Invitrogen; Carlsbad, CA), 1:400 in 1% BSA-PBS solution followed by PBS washing. The nuclei of attached cells were then stained by incubation with Hoechst 33342 trihydrochloride, trihydrate (2 μg/mL) (Invitrogen; Carlsbad, CA) for 5 min at room temperature followed by PBS washing. Following staining the media chambers were removed from the chamber slide systems. A coverslip was mounted onto the glass with faramount aqueous mounting medium (DakoCytomation; Carpinteria, CA). Immunofluorescence-labeled cells were observed with an inverted confocal microscope (LSM 510; Carl Zeiss MicroImaging Inc., Thornwood, NY) equipped with two lasers used simultaneously: a diode laser (excitation wavelength 405 nm) and a diode-pumped solid state laser (excitation wavelength 561 nm). The objective was an immersion oil plan-neofluor 63x/1.4 (Carl Zeiss Microimaging Inc., Thornwood, NY). For FA morphometry, optical sections of 1024 × 1024 pixels were acquired. Image acquisition and control was accomplished using Zeiss imaging software (version 4.2; Zeiss LSM 510, Carl Zeiss MicroImaging GmbH, Germany). Images were subsequently analyzed using NIH ImageJ software. The length of vinculin-stained FA was determined by their longest axis regardless of orientation. A minimum of 10 FA for 10 different cells in each group were identified and measured from each experiment (22).

In vitro Adhesion Assay

Briefly, OPN was diluted to 50 nM in carbonate buffer (pH 9.6), and 50 μl/well was added to 96-well EIA/RIA high binding plates (Corning Inc.; Corning, NY) and placed overnight at 4ºC. Wells were rinsed with PBS, and non-specific binding sites were blocked via the addition of 1% BSA in PBS for 1 h at 37ºC. Human dermal fibroblasts grown to confluence under the conditions described above were resuspended in DMEM serum-free medium at a concentration of 3×10^6 cells/ml. In addition resuspended cells were treated with 30 μM Calcein-AM (EMD; Gibbstown, NJ) for 30 min at 37ºC and 5% CO_2 for adhesion analysis. Cells were washed with Hanks Balanced Salt Solution (HBSS) (Invitrogen; Carlsbad, CA) and resuspended in DMEM serum-free medium containing treatment conditions (OPN-R3, FBS, or DMEM alone) and plated into wells at 1×10^5 cells/well (100 μl/well). Adhesion was allowed to proceed for 1 h at 37ºC and 5% CO_2. Non-adherent cells in the supernatant were removed from each well via aspiration. Each well was washed twice with HBSS, then 100 μl of HBSS was then added each well. The plate was then covered with packing tape, inverted, centrifuged at 200g for 5 min to remove weakly adherent cells, and100 μl of HBSS was added to each well before the plate was read on a fluorescence plate reader at 485/538 nm wave length. Experiment was performed in triplicate with fibroblasts from a single human patient.

In vitro Proliferation Assay

Proliferation was assessed using a CellTiter 96® AQ_{ueous} Non-Radioactive Cell Proliferation Assay (Promega Corporation; Madison, WI). Briefly, human dermal fibroblasts grown to confluence under the conditions described above were resuspended in DMEM with 10% FBS at a concentration of 1×10^4cells/ml. Cells were plated at 2×10^3 cells/well (200 μl) on a 96 well Microtest tissue culture plate (Becton Dickinson and Co.; Franklin Lakes, NJ) in DMEM with 10% FBS for 24 h at 37ºC and 5% CO_2. After 24 h under normal conditions cells were washed with PBS, and serum starved overnight. Following serum starvation, treatment conditions (18.75 nM OPN, OPN-R3, DMEM, FBS) were added and cells were incubated for 24 h at 37ºC and 5% CO_2. Following 24 h treatment with experimental conditions 20 μl of MTS (3-(4,5-dimethylthiazol-2-yl)-5-(3-carboxymethoxyphenyl)-2-(4-sulfophenyl)-2H-tetrazolium, inner salt, Promega Corporation; Madison, WI) was added to each well. The plate was then incubated at 37ºC and 5% CO_2 and the absorbance at 490 nm wavelength was recorded using an ELISA plate reader at 1 h intervals over a period of 4 h. The change in absorbance is indicative of the cellular reduction of MTS and thus cellular proliferation.

In vitro Free-Floating Collagen Lattice Assay

Fibroblast populated collagen lattices are frequently used as a contraction model (23). Collagen lattices are a model system for studying the cellular mechanisms of tension generation by cells in an extracellular matrix and have been used to study different agonists and antagonists, different cell types and different contractile pathological conditions for example wound healing, scar and Dupuytren's contracture and aging (24, 25) (26, 27) (28) (29). Briefly, in this model cultured human dermal fibroblasts are suspended in a rapidly polymerizing collagen matrix to produce the fibroblast-populated collagen lattice. With time, this lattice will undergo a reduction in size referred to as lattice contraction. Cell contractility was assessed using a previously described protocol with slight modifications (30). Briefly, non-specific binding sites of 48 well tissue culture treated plates (Corning Inc.; Corning, NY) were blocked by the addition of 1% BSA for 1 h at 37ºC and allowed to dry overnight. On the following day human dermal fibroblasts grown to confluence under the conditions described above, were resuspended in DMEM serum-free medium at a concentration of 1×10^6 cells/ml. Under sterile conditions, a collagen solution was prepared from 0.3 ml of 5× PBS, 1.3 ml of 6.4 mg/ml purified collagen (Nutragen; Fremont, CA), 8 ml of DMEM, and 0.5 ml of cell suspension. This collagen solution was incubated in a water bath at 37ºC for 3 min before 160 μl of this solution was added to the wells of a previously BSA blocked plate. The plate was incubated at for 2 h at 37ºC and 5% CO_2 to allow the collagen to polymerize, the collagen lattices were then gently freed by tilting the plates, and 160 μl of DMEM containing the appropriate concentrations of test substances (OPN, OPN-R3, DMEM, and FBS) was added to the well. Lattice contraction was measured using a digital scanner every 4 h for the first 12 h, then every 12 h until contraction was no longer observed. Images were subsequently analyzed using NIH ImageJ software.

Immunohistochemistry

Formalin fixed and paraffin embedded tissues were obtained from DUMC, Department of Pathology repository of tissue specimens in accordance with the DUMC Institutional Review Board. Selection of specimens was based on the age of the scar so that the scars would either be in the remodeling phase of repair, which beings on post-operative day fourteen and can continue for up to two years, or after the remodeling phase of repair. Scar re-excisions ranged from postoperative 14d to 1058d (table 1). A sample section of the tissue was stained by hematoxylin and eosin, and reviewed a under light microscope for the presence of the scar and normal tissue within the section. Samples were selected to match for patient's race, gender, age and scar location. Specimens were equivalent across groups

($p \geq 0.05$) except for gender. Human scar tissue of consecutive sections of 5μm was immunostained for OPN. Sections were incubated for 45min with the rabbit, anti-OPN (Abcam, Cambridge MA.), at 1:200 dilution. Tissue staining was visualized using the avidin biotinylated enzyme complex system (Vectastain Elite ABC, Vector. Burlingame, Ca.) and 3,3′-Diaminobenzidine substrate chromogen solution (Dako, Carpinteria, CA). To quantify the degree of positive staining for OPN, each slide was subjected to semi-quantitative anlaysis using the following system: 0, 1 (0–25% reactivity), 2 (35–50% reactivity), 3 (50–75% reactivity), and 4 (75–100% reactivity).

Statistical Analysis

Data are presented as the mean ± SEM. All *in vitro* assays were analyzed for statistical significance using one-way analysis of variance (ANOVA). Statistical significance for this study is set at $p \leq 0.05$.

RESULTS

Effects of OPN on Human Dermal Fibroblast Cell Migration

To examine the effect of osteopontin on human dermal fibroblast cell migration, we used modified Boyden chambers (19). The number of cells that migrated in the absence of OPN was used as a baseline cellular migration. As shown in Figure 1, after a 22 h incubation at 37ºC and 5% CO_2, human dermal fibroblasts significantly moved toward OPN (18.75 nM) to a greater extent than they did toward the control in the lower chamber. OPN increased fibroblast migration greater than 3-fold ($p \leq 0.01$; 309.62% ± 11.90% *versus* 100% ± 3.28%). The migration of human dermal fibroblasts toward OPN was significantly inhibited by the addition of OPN-R3 (187.5 nM) to the upper chamber ($p \leq 0.01$; 309.62% ± 11.90% *versus* 125.70% ± 12.89%).

Effects of OPN on Human Dermal Fibroblast FA Length

To determine the effect of OPN on FA length, four different cell lines of normal human dermal fibroblasts were cultured overnight on non-treated glass, glass treated with 50 nM OPN alone, or 50 nM OPN and 500 nM OPN-R3. Images of fluorescent stained fibroblasts and measurements of the lengths of FAs are presented in Figure 2. Fibroblast FA length was not increased in the presence of OPN. There was no statistical difference in FA length between groups ($p > 0.05$; 4.72 μm ± 0.25 μm *versus* 4.42 μm ± 0.19 μm *versus* 4.63 μm ± 0.37 μm).

Effects of OPN on Human Dermal Fibroblast Cell Adhesion

To investigate whether OPN induced stronger cell attachment to substrate, we used a previously established *in vitro* cell adhesion assay (19). The fluorescent readings in the 1% BSA coating and OPN-R3 alone coating were used as controls. Figure 3 shows that after 1 h incubation at 37ºC and 5% CO_2, OPN propagates human dermal fibroblast adhesion by greater than 20-fold ($p \leq 0.05$; 126.00 ± 7.54 *versus* 4.45 ± 3.04). The increase in cell adhesion despite no change in FA length suggest that a mechanism other than simply increasing FA size is responsible for the strength of interaction between human dermal fibroblasts and the underlying substrate. Adhesiveness of fibroblasts to OPN was significantly inhibited by addition of OPN-R3 ($p \leq 0.05$; 126.00 ± 7.54 *versus* 21.89 ± 1.50).

Effects of OPN on Human Dermal Fibroblast Proliferation

To investigate the effects of OPN on human dermal fibroblast proliferation, a previously established CellTiter 96® AQ_{ueous} Non-Radioactive Cell Proliferation assay was utilized. Proliferation in the FBS group served as a control for maximum proliferation in the presence

of serum, while the 0 nM OPN group was used a control for baseline proliferation in the absence of serum and OPN. As shown in Figure 4A, after 24 h incubation at 37ºC and 5% CO_2, human dermal fibroblasts proliferation was significantly increased in the presence of OPN compared to baseline control ($p \leq 0.05$; 100% ± 4.26% *versus* 144.42% ± 5.91% at 12.5 nM OPN, $p \leq 0.05$; 100% ± 4.26% *versus* 146.10% ± 12.9% at 25 nM OPN, $p \leq 0.05$; 100% ± 4.26% *versus* 144.42% ± 9.67% at 50 nM OPN); however, there was no significant difference amongst the OPN treated groups. While not significantly different, 100 nM OPN appeared to decrease proliferation towards baseline when compared to the other OPN concentrations. As seen in Figure 4B, OPN-induced proliferation was significantly inhibited in the presence of OPN-R3 at all concentrations ($p \leq 0.05$; 100.00% ± 4.29% *versus* 74.78% ± 6.12% at 2.5X OPN-R3, $p \leq 0.05$; 100.00% ± 4.29% *versus* 78.48% ± 3.95% at 5X OPN-R3, $p \leq 0.05$; 100.00% ± 4.29% *versus* 77.10% ± 6.09% at 10X OPN-R3, $p \leq 0.05$; 100.00% ± 4.29% *versus* 73.59% ± 4.60% at 50X OPN-R3). OPN-R3 had no baseline effect on proliferation in the absence of OPN.

Effects of OPN on Human Dermal Fibroblast Contractility

To examine the effect of OPN on human dermal fibroblast contractility, we utilized free floating collagen lattices. The contractility seen in the absence of OPN and FBS was used as a control for baseline contractility. The FBS group was a positive control for serum induced-contractility. As shown in Figure 5, the OPN (18.75 nM) treated group had a significant increase in contractility when compared to the non-OPN treated group ($p \leq 0.05$; 0.075 cm^2 ± 0.009 cm^2 *versus* 0.118 cm^2 ± 0.025 cm^2). In addition, OPN-induced contractility was significantly decreased in the presence of OPN-R3 that is 50–100x as concentrated as OPN ($p \leq 0.05$; 0.075 cm^2 ± 0.009 cm^2 *versus* 0.126 cm^2 ± 0.006 cm^2 at 50X OPN-R3, $p \leq 0.05$; 0.075 cm^2 ± 0.009 cm^2 *versus* 0.111 cm^2 ± 0.002 cm^2 at 100X OPN-R3).

Immunohistochemistry of Scar and Normal Tissue

To examine the expression patterns of OPN in scar and normal tissue Immunohistochemistry was utilized. Immunohistology staining of human scar tissue shows increased OPN expression compared to normal tissue. As shown in Fig 6, an eighty-four day old scar stained more robustly for OPN, primarily in fibroblast than surrounding normal tissue. This immunohistology staining is a typical representation of OPN staining found in 10 scar samples. To quantify the degree of positive staining for OPN, each slide was subjected to semi-quantitative anlaysis. Table 2 demonstrates that scar tissue was significantly stained for OPN. OPN staining was found to increase with increasing scar age, then decrease as cellularity resolved in scars over 2 years old that were not long in the remodeling phase. This staining pattern demonstrates the relationship between OPN and scar.

DISCUSSION

OPN is a multifunctional cytokine and adhesion molecule known to be involved in an array of biological processes including bone remodeling, cancer metastasis, inflammation, and scarring (7, 11, 12, 16). In this study we focused on the nature of the human dermal fibroblast response to OPN, as well as the ability of the OPN specific RNA aptamer, OPN-R3, to ablate OPN-induced responses. The results of these studies provide insight into establishing the role of OPN in dermal fibrosis and scar formation as well as the role of OPN-R3 in preventing fibrosis and scarring.

Previous studies examining organ fibrosis have demonstrated that OPN exerts pro-fibrotic effects (18, 31, 32). Studies investigating human idiopathic pulmonary fibrosis determined that OPN induces both lung fibroblast migration and proliferation (17). The studies

involving lung fibroblasts are useful in helping to decipher the role of OPN throughout the human body; however, there is a still a gap in the knowledge regarding how OPN affects key cells in dermal wound healing and scarring, such as human dermal fibroblasts. The experiments of the current study filled this knowledge gap by studying the pro-fibrotic effects of OPN on human dermal fibroblasts. In this study, we demonstrate that (1) OPN strongly mediates dermal fibroblast migration, adhesion, proliferation, and contractility, (2) OPN induced effects are inhibited in the presence of OPN-R3, and (3) OPN does not affect FA size.

Our studies show that OPN is indeed involved in dermal scarring and that its presence induces dermal fibroblast activation, more specifically inducing fibroblast migration, adhesion, proliferation, and contractility. The IHC staining pattern seen when scar tissue is compared to normal tissue demonstrates the key relationship between OPN and scar fibroblasts. This relationship highlights the likelihood that OPN is involved in fibrosis. The cellular response to OPN suggests that OPN may in fact exert is pro-fibrotic effects through its interactions with dermal fibroblasts. Fibroblast migration, proliferation, and decreased apoptosis contribute to the accumulation and expansion of fibroblastic foci which may represent the “leading edge” of the progressive fibrotic process (33–35). OPN interaction with cell surface receptors, particularly $\alpha_v\beta_3$-integrin is believed to be primarily responsible for adhesion, migration, proliferation, and cytoskeletal organization (13). It is has been suggested that OPN binding to $\alpha_v\beta_3$-integrin leads to phosphorylation of focal adhesion kinase (FAK), paxillin, tensin, and Src, which activate downstream pathways that ultimately terminate in specific cellular responses (13, 36). Studies examining lung fibroblasts confirm that migration and proliferation are dependent on OPN interaction with $\alpha_v\beta_3$-integrin. Interestingly, those studies also show that OPN has pro-fibrotic effects on molecules involved in extracellular matrix (ECM) remodeling. Pardo et. al determined that, in lung fibroblasts, OPN interaction with CD44 increased TIMP-1 (tissue inhibitor of metalloproteinase-1) and type I collagen while inhibiting MMP-1 (matrix metalloproteinase-1) (17). This results in the accumulation of ECM and inhibition of type I collagen degradation (17, 37, 38). Such a shift in the balance of ECM maintenance has significant effects on lung fibrosis. It is possible that similar events occur with dermal fibroblasts and dermal fibrosis, although it has not been investigated. We have shown that OPN induces migration, proliferation, and adhesion. The pro-fibrotic environment of accumulated dermal fibroblasts with an absence of ECM degradation provides a possible explanation for the role of OPN in dermal fibrosis and scar formation; however, further experiments will be needed to determine this point. OPN increased dermal fibroblast contractility in comparison to controls. The free floating collagen lattices used in these experiments are representative of the mechanically relaxed tissue seen in early wound healing where tensile strength is low (30, 39). While the exact mechanisms for increasing cell contractility in response to OPN are not known several possibilities can be considered. OPN binding to $\alpha_v\beta_3$-integrin can produce changes in cytoskeletal organization by way of FAK activation (13). OPN binding to $\alpha_v\beta_3$-integrin is also known to increase intracellular Ca^{2+} levels from intracellular compartments and via extracellular influx (13, 40, 41). It is possible that the increase in intracellular Ca^{2+} activates calmodulin which then activates MLCK which leads to increased cell contractility. When considering possibilities for increased contractility one must also consider possible up-regulation of α-smooth muscle actin or other microfilaments that may be involved in cell contractility. These mechanisms are all potential means by which OPN induces increased dermal fibroblast contractility and further investigation will be needed to determine which pathways are involved.

Previous studies have utilized antisense oligonucleotides to block OPN and its effects. *In vivo* rodent wound studies using antisense oligodeoxynucleotides to create OPN knockdowns determined that OPN knockdown dermal wounds had a considerably reduced

cross-sectional area of granulation tissue compared to controls, thereby implicating OPN as a partial cause of the extensive granulation tissue formation and subsequent fibrosis. This was the first study to examine OPN and dermal fibrosis (42). While the results of this study are notable, the use of antisense oligonucleotides is restricted to intracellular applications. In contrast, RNA aptamers can effectively target extracellular targets, such as OPN (11). RNA aptamers, as a class of therapeutics are becoming increasingly useful due to their specificity and lack of immunogenicity. One example of RNA aptamer technology being utilized in an actual clinical setting is pegaptanib, which was recently approved for age-related macular degeneration treatment (11). With the potential to eventually be translated from basic science to clinical therapy the effectiveness of the OPN specific RNA aptamer, OPN-R3, was evaluated as a pre-clinical candidate.

The results of this study show that OPN-R3 significantly reduces the effects of OPN on human dermal fibroblasts *in vivo*. While the exact mechanisms responsible for the pro-fibrotic effects of OPN are not fully understood at this time, the possibility that OPN-R3 could be applied to wounds as a means to decrease scarring and fibrosis is intriguing. This study suggests that OPN-R3 may serve as an anti-fibrotic by decreasing fibroblast migration, adhesion, and proliferation in dermal wounds. At this time it is not clear whether OPN-R3 effects are due to decreased cell signaling or some other mechanism. Future studies will be needed to address this question. It is known that in the absence of OPN, wounds heal with normal tensile strength; however, there is decreased debridement, and greater ECM disorganization. Wounds of OPN-null mice maintain smaller diameter collagen type III fibers in a disorganized matrix (20). Normal wound maturation involves a transition from collagen type III to collagen type I, the same collagen type noted to be involved in fibrosis. Another possible mechanism for OPN-R3 to prevent scar formation is to prevent normal wound maturation via ECM turnover. Further experiments will be necessary to fully understand the functions of OPN in dermal wound healing.

Despite the OPN-induced increased in adhesion seen in this study, there is no change in FA length in response to OPN. These results encourage further study to determine other mechanisms that could be responsible for the increase in cell adhesion in the presence of OPN. One possibility involves exploring cell signaling pathways. OPN is known to interact with $\alpha_v\beta_3$-integrin and activate FAK which then activates downstream pathways. Future studies will evaluate these pathways by using *in vitro* studies such as western blot analysis to analyze relative levels of signaling molecules including FAK, ROCK, Rho GTPases, and MRLC in the presence and absence of OPN.

Our results support the hypothesis that (1) OPN promotes dermal fibrosis by increasing dermal fibroblast motility, focal adhesion length, adhesion, proliferation, and contractility, and that (2) OPN induced effects are significantly inhibited in the presence of the OPN-R3 RNA, with the exception of OPN increasing FA length.

There are several studies supporting the use of *in vitro* assays to characterize cellular response to OPN. This study is significant because using these *in vitro* assays to characterize the human dermal fibroblast response to OPN is novel. The results of these studies suggests that OPN is involved in dermal fibrosis and scar formation, and although the exact mechanisms are not known OPN, at least partially, promotes its pro-fibrotic effects via increasing dermal fibroblast motility, adhesion, proliferation, and contractility. OPN may eventually be used as a therapy for non-healing wounds such as those seen in diabetic patients. *In vivo* studies using diabetic model mice have demonstrated that non-diabetic mice wounds have higher levels of OPN in the first few days post-wounding when compared to diabetic mice (43). They also show that OPN expression was correlated with the extent of wound healing. The delay in wound healing associated with the delay in OPN

expression suggests that low levels of OPN may be responsible for the delayed wound healing of diabetic mice (43). Likewise, OPN-R3 may eventually be used as an alternative means to treat and prevent fibrosis and scar formation due to the anti-fibrotic effects demonstrated in this study.

In summary, in this study we highlight the role of OPN in promoting dermal fibrosis and scarring, and the role of OPN-R3 in reducing dermal fibrosis and scarring. Although previous studies have suggested that OPN has pro-fibrotic effects in organs such as the lung and kidney, its role in dermal fibrosis and scarring was unclear. We demonstrated that OPN increases dermal fibroblast motility, adhesion, proliferation, and contractility. We demonstrated that OPN-R3 significantly inhibits OPN-induced effects. Our results suggest a mechanism explaining at least a portion of the pro-fibrotic effects of OPN by its direct effects on human dermal fibroblasts. Our results regarding OPN-R3 inhibiting OPN-induced effects highlights OPN-R3 as a potential therapeutic intervention in dermal fibrosis and scar formation. We are interested in translating our basic science work to the clinical setting. To continue this process future studies will involve (1) investigating how OPN affects molecules in the ECM such as collagen type 1, TIMP-1, and MMP-1, (2) investigating key signaling pathways and their response to OPN, these will include ROCK, Rho GTPases, MRLC, and FAK, and (3) using biomimetics and nanotechnology to develop reliable methods of delivering OPN and OPN-R3 to animal models of non-healing diabetic wounds and fibrosis wounds for *in vivo* studies such as open wound healing (44).

Acknowledgments

This work was supported by the Howard Hughes Medical Institute Medical Student Fellowship program, a Gardner Award from the Duke Department of Surgery, and a NIH K08 Career Scientist Development Award.

References

1. Bush J, So K, Mason T, Occleston NL, O'Kane S, Ferguson MW. Therapies with emerging evidence of efficacy: avotermin for the improvement of scarring. Dermatol Res Pract. 2010:2010.
2. Lee MY, Ehrlich HP. Influence of vanadate on migrating fibroblast orientation within a fibrin matrix. J Cell Physiol. 2008; 217:72–76. [PubMed: 18498123]
3. Miyazaki K, Okada Y, Yamanaka O, et al. Corneal wound healing in an osteopontindeficient mouse. Invest Ophthalmol Vis Sci. 2008; 49:1367–1375. [PubMed: 18385052]
4. Stramer BM, Mori R, Martin P. The inflammation-fibrosis link? A Jekyll and Hyde role for blood cells during wound repair. J Invest Dermatol. 2007; 127:1009–1017. [PubMed: 17435786]
5. Jun JI, Lau LF. The matricellular protein CCN1 induces fibroblast senescence and restricts fibrosis in cutaneous wound healing. Nat Cell Biol. 2010; 12:676–685. [PubMed: 20526329]
6. Liaw L, Skinner MP, Raines EW, et al. The adhesive and migratory effects of osteopontin are mediated via distinct cell surface integrins. Role of alpha v beta 3 in smooth muscle cell migration to osteopontin in vitro. J Clin Invest. 1995; 95:713–724. [PubMed: 7532190]
7. O'Regan A, Berman JS. Osteopontin: a key cytokine in cell-mediated and granulomatous inflammation. Int J Exp Pathol. 2000; 81:373–390. [PubMed: 11298186]
8. Denhardt DT, Guo X. Osteopontin: a protein with diverse functions. Faseb J. 1993; 7:1475–1482. [PubMed: 8262332]
9. Singh K, DeVouge MW, Mukherjee BB. Physiological properties and differential glycosylation of phosphorylated and nonphosphorylated forms of osteopontin secreted by normal rat kidney cells. J Biol Chem. 1990; 265:18696–18701. [PubMed: 2211731]
10. Buback F, Renkl AC, Schulz G, Weiss JM. Osteopontin and the skin: multiple emerging roles in cutaneous biology and pathology. Exp Dermatol. 2009; 18:750–759.21. [PubMed: 19558497]
11. Mi Z, Guo H, Russell MB, Liu Y, Sullenger BA, Kuo PC. RNA aptamer blockade of osteopontin inhibits growth and metastasis of MDA-MB231 breast cancer cells. Mol Ther. 2009; 17:153–161. [PubMed: 18985031]

12. Denhardt DT, Noda M, O'Regan AW, Pavlin D, Berman JS. Osteopontin as a means to cope with environmental insults: regulation of inflammation, tissue remodeling, and cell survival. J Clin Invest. 2001; 107:1055–1061. [PubMed: 11342566]

13. Sodek J, Ganss B, McKee MD. Osteopontin. Crit Rev Oral Biol Med. 2000; 11:279–303. [PubMed: 11021631]

14. Craig SW, Johnson RP. Assembly of focal adhesions: progress, paradigms, and portents. Curr Opin Cell Biol. 1996; 8:74–85. [PubMed: 8791409]

15. Lopez CA, Davis RL, Mou K, Denhardt DT. Activation of a signal transduction pathway by osteopontin. Ann N Y Acad Sci. 1995; 760:324–326. [PubMed: 7540377]

16. Miyazaki K, Okada Y, Yamanaka O, et al. Corneal wound healing in an osteopontin-deficient mouse. Investigative ophthalmology & visual science. 2008; 49:1367–1375. [PubMed: 18385052]

17. Pardo A, Gibson K, Cisneros J, et al. Up-regulation and profibrotic role of osteopontin in human idiopathic pulmonary fibrosis. PLoS Med. 2005; 2:e251. [PubMed: 16128620]

18. Persy VP, Verhulst A, Ysebaert DK, De Greef KE, De Broe ME. Reduced postischemic macrophage infiltration and interstitial fibrosis in osteopontin knockout mice. Kidney Int. 2003; 63:543–553. [PubMed: 12631119]

19. Takahashi F, Takahashi K, Okazaki T, et al. Role of osteopontin in the pathogenesis of bleomycin-induced pulmonary fibrosis. Am J Respir Cell Mol Biol. 2001; 24:264–271. [PubMed: 11245625]

20. Liaw L, Birk DE, Ballas CB, Whitsitt JS, Davidson JM, Hogan BL. Altered wound healing in mice lacking a functional osteopontin gene (spp1). J Clin Invest. 1998; 101:1468–1478. [PubMed: 9525990]

21. Mi Z, Guo H, Kuo PC. Identification of osteopontin-dependent signaling pathways in a mouse model of human breast cancer. BMC Res Notes. 2009; 2:119. [PubMed: 19570203]

22. Dugina V, Fontao L, Chaponnier C, Vasiliev J, Gabbiani G. Focal adhesion features during myofibroblastic differentiation are controlled by intracellular and extracellular factors. J Cell Sci. 2001; 114:3285–3296. [PubMed: 11591817]

23. Carlson MA, Longaker MT. The fibroblast-populated collagen matrix as a model of wound healing: a review of the evidence. Wound Repair Regen. 2004; 12:134–147. [PubMed: 15086764]

24. Mirastschijski U, Schnabel R, Claes J, et al. Matrix metalloproteinase inhibition delays wound healing and blocks the latent transforming growth factor-β1-promoted myofibroblast formation and function. Wound Repair and Regeneration. 2010; 18:223–234. [PubMed: 20409148]

25. Vaughan MB, Howard EW, Tomasek JJ. Transforming Growth Factor-[beta]1 Promotes the Morphological and Functional Differentiation of the Myofibroblast. Experimental Cell Research. 2000; 257:180–189. [PubMed: 10854066]

26. Komatsu I, Bond J, Selim A, Tomasek JJ, Levin LS, Levinson H. Dupuytren's Fibroblast Contractility by Sphingosine-1-Phosphate Is Mediated Through Non-Muscle Myosin II. The Journal of Hand Surgery. 2010; 35:1580–1588. [PubMed: 20888494]

27. Dallon JC, Ehrlich HP. Differences in the mechanism of collagen lattice contraction by myofibroblasts and smooth muscle cells. Journal of Cellular Biochemistry. 2010; 111:362–369. [PubMed: 20506308]

28. Zhang Z, Garron TM, Li X-J, et al. Recombinant human decorin inhibits TGF-[beta]1-induced contraction of collagen lattice by hypertrophic scar fibroblasts. Burns. 2009; 35:527–537. [PubMed: 19167828]

29. Treiber N, Peters T, Sindrilaru A, et al. Overexpression of manganese superoxide dismutase in human dermal fibroblasts enhances the contraction of free floating collagen lattice: implications for ageing and hyperplastic scar formation. Archives of Dermatological Research. 2009; 301:273–287.22. [PubMed: 19306099]

30. Arora PD, Narani N, McCulloch CA. The compliance of collagen gels regulates transforming growth factor-beta induction of alpha-smooth muscle actin in fibroblasts. Am J Pathol. 1999; 154:871–882. [PubMed: 10079265]

31. Trueblood NA, Xie Z, Communal C, et al. Exaggerated left ventricular dilation and reduced collagen deposition after myocardial infarction in mice lacking osteopontin. Circ Res. 2001; 88:1080–1087. [PubMed: 11375279]

32. Matsui Y, Jia N, Okamoto H, et al. Role of osteopontin in cardiac fibrosis and remodeling in angiotensin II-induced cardiac hypertrophy. Hypertension. 2004; 43:1195–1201. [PubMed: 15123578]
33. Crystal RG, Bitterman PB, Mossman B, et al. Future research directions in idiopathic pulmonary fibrosis: summary of a National Heart, Lung, and Blood Institute working group. Am J Respir Crit Care Med. 2002; 166:236–246. [PubMed: 12119236]
34. Kuhn C. Patterns of lung repair. A morphologist's view. Chest. 1991; 99:11S–14S. [PubMed: 1997262]
35. Kuhn C 3rd, Boldt J, King TE Jr, Crouch E, Vartio T, McDonald JA. An immunohistochemical study of architectural remodeling and connective tissue synthesis in pulmonary fibrosis. Am Rev Respir Dis. 1989; 140:1693–1703. [PubMed: 2604297]
36. Frisch SM, Vuori K, Ruoslahti E, Chan-Hui PY. Control of adhesion-dependent cell survival by focal adhesion kinase. J Cell Biol. 1996; 134:793–799. [PubMed: 8707856]
37. Selman M, Ruiz V, Cabrera S, et al. TIMP-1, -2, -3, and -4 in idiopathic pulmonary fibrosis. A prevailing nondegradative lung microenvironment? Am J Physiol Lung Cell Mol Physiol. 2000; 279:L562–574. [PubMed: 10956632]
38. Kolb M, Bonniaud P, Galt T, et al. Differences in the fibrogenic response after transfer of active transforming growth factor-beta1 gene to lungs of "fibrosis-prone" and "fibrosisresistant" mouse strains. Am J Respir Cell Mol Biol. 2002; 27:141–150. [PubMed: 12151305]
39. Grinnell F. Fibroblasts, myofibroblasts, and wound contraction. J Cell Biol. 1994; 124:401–404. [PubMed: 8106541]
40. Miyauchi A, Alvarez J, Greenfield EM, et al. Recognition of osteopontin and related peptides by an alpha v beta 3 integrin stimulates immediate cell signals in osteoclasts. J Biol Chem. 1991; 266:20369–20374. [PubMed: 1939092]
41. Zimolo Z, Wesolowski G, Tanaka H, Hyman JL, Hoyer JR, Rodan GA. Soluble alpha v beta 3-integrin ligands raise [Ca2+]i in rat osteoclasts and mouse-derived osteoclast-like cells. Am J Physiol. 1994; 266:C376–381. [PubMed: 8141251]
42. Mori R, Shaw TJ, Martin P. Molecular mechanisms linking wound inflammation and fibrosis: knockdown of osteopontin leads to rapid repair and reduced scarring. J Exp Med. 2008; 205:43–51. [PubMed: 18180311]
43. Sharma A, Singh AK, Warren J, Thangapazham RL, Maheshwari RK. Differential regulation of angiogenic genes in diabetic wound healing. J Invest Dermatol. 2006; 126:2323–2331. [PubMed: 16874314]
44. Andreadis ST, Geer DJ. Biomimetic approaches to protein and gene delivery for tissue regeneration. Trends Biotechnol. 2006; 24:331–337. [PubMed: 16716420]

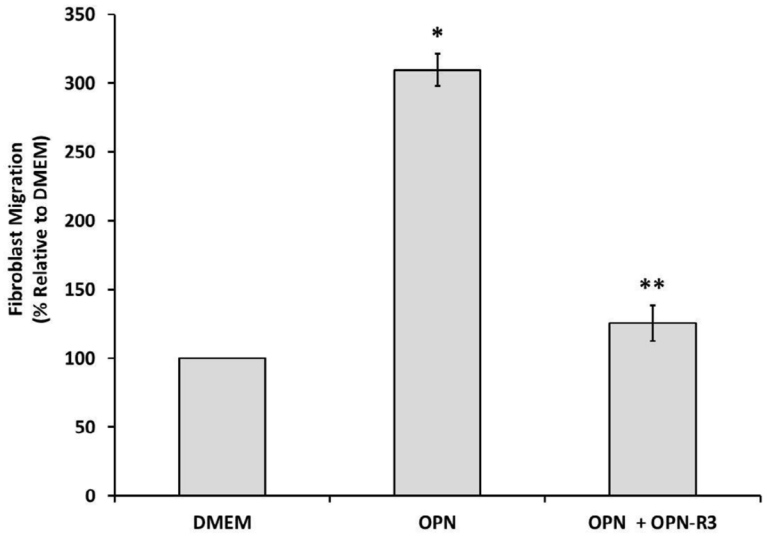

Figure 1.

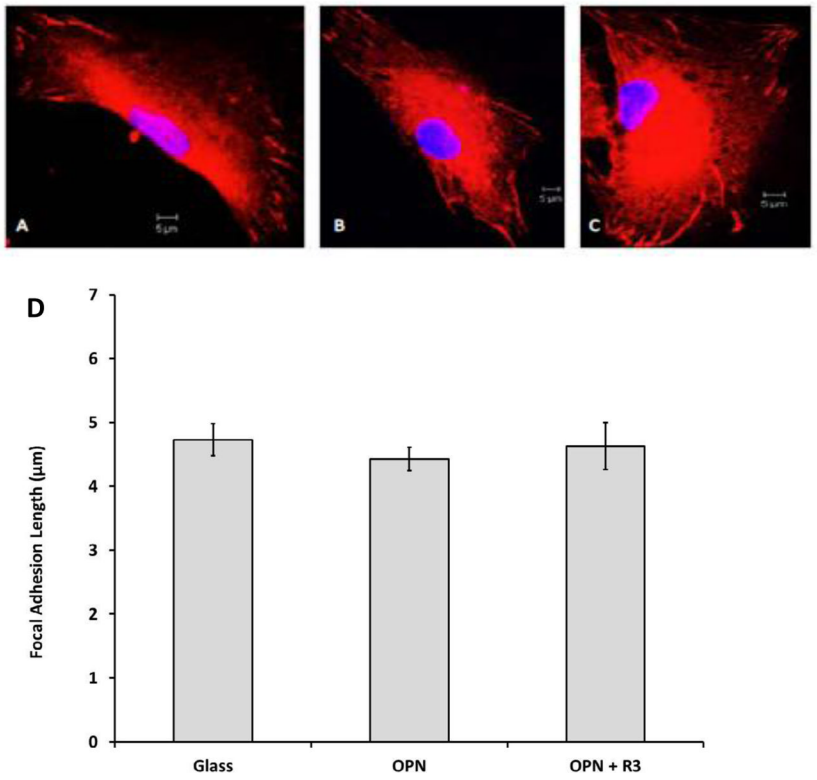

Figure 2.

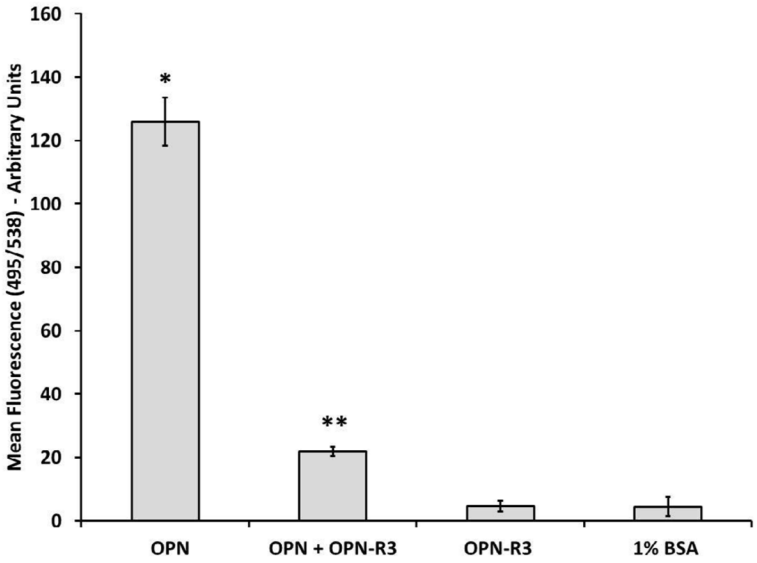

Figure 3.

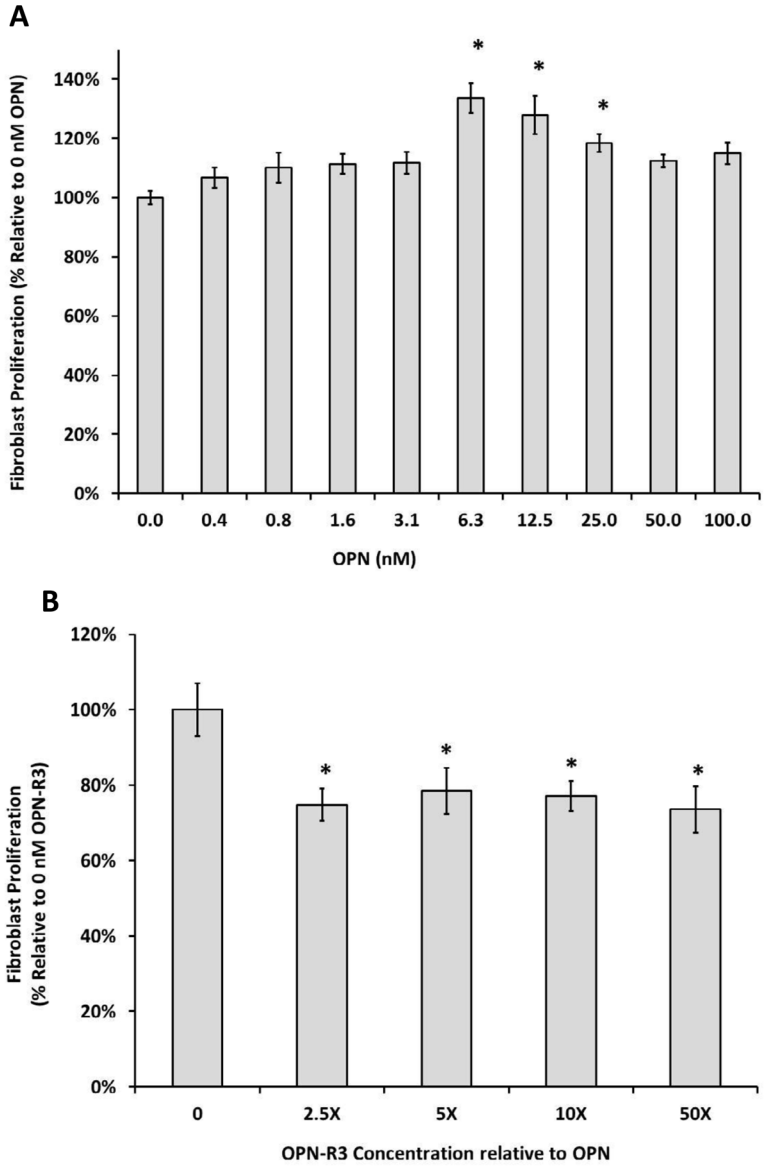

Figure 4.

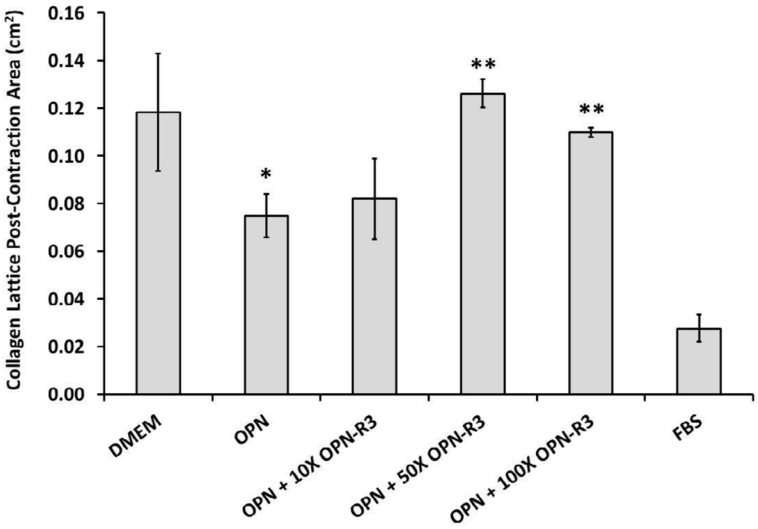

Figure 5.

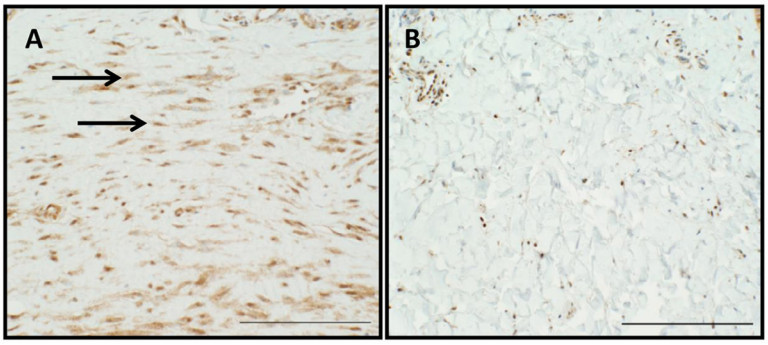

Figure 6.

Table 1

Patient Demographic of Selected Scar Samples

Group	N
Race	
Caucasian	9
Black	0
Gender	
Male	4
Female	5
Age (years)	
<50	3
>50	6
Scar location	
Head	1
Trunk	5
Upper extremities	1
Lower extremities	2
Scar Age	
2wks–6mos	**6**
Male	3
Female	3
>6 mos	**3**
Male	1
Female	2

Table 2

Semi-quantitative analysis of OPN expression in scar and normal tissue. Scar tissue expressed more OPN than normal tissue. Scar tissue that scored in the lower percentiles were not in the active remodeling phase and had decreased cellularity. p=0.001.

	Scar	Normal
0–25%	1	7
25–50%	1	2
50–75%	0	0
75–100%	7	0